Science of the Total Environment 571 (2016) 1330–1339

Contents lists available at ScienceDirect

Science of the Total Environment

journal homepage: www.elsevier.com/locate/scitotenv

Global assessment of heat wave magnitudes from 1901 to 2010 and implications for the river discharge of the Alps

Matteo Zampieri [a,*], Simone Russo [b], Silvana di Sabatino [c], Melania Michetti [d], Enrico Scoccimarro [e], Silvio Gualdi [e]

[a] Euro Mediterranean Center on Climate Change (CMCC), Bologna University, Bologna, Italy
[b] Joint Research Center (JRC), Ispra, Italy
[c] Bologna University, Italy
[d] CMCC, Italy
[e] CMCC, National Institute of Geophysics and Volcanology (INGV), Bologna, Italy

HIGHLIGHTS

- The 20th Century Reanalyses allow identifying of several undocumented heat waves of the past.
- Recently, significant heat wave patterns have emerged on a global scale.
- Water availability in Europe may decline in the future.

GRAPHICAL ABSTRACT

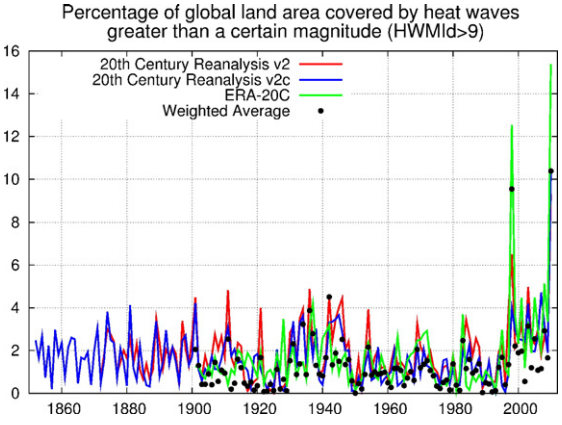

ARTICLE INFO

Article history:
Received 15 April 2016
Received in revised form 1 July 2016
Accepted 1 July 2016
Available online 11 July 2016

Editor: Dr. D. Barcelo

Keywords:
20th century reanalysis
Heat waves
Alps

ABSTRACT

Heat waves represent one of the most significant climatic stressors for ecosystems, economies and societies. A main topic of debate is whether they have increased or not in intensity and/or their duration due to the observed climate change. Firstly, this is because of the lack of reliable long-term daily temperature data at the global scale; secondly, because of the intermittent nature of such phenomena. Long datasets are required to produce a reliable and meaningful assessment. In this study, we provide a global estimate of heat wave magnitudes based on the three most appropriate datasets currently available, derived from models and observations (i.e. the 20th Century Reanalyses from NOAA and ECMWF), spanning the last century and before. The magnitude of the heat waves is calculated by means of the Heat Wave Magnitude Index daily (HWMId), taking into account both duration and amplitude.

We compare the magnitude of the most severe heat waves occurred across different regions of the world and we discuss the decadal variability of the larger events since the 1850s. We concentrate our analysis from 1901 onwards, where all datasets overlap. Our results agree with other studies focusing on heat waves that have occurred

* Corresponding author.
E-mail addresses: matteo.v.zampieri@gmail.com, matteo.zampieri@cmcc.it, matteo.zampieri2@unibo.it (M. Zampieri), simone.russo@jrc.ec.europa.eu (S. Russo), silvana.disabatino@unibo.it (S. di Sabatino), melania.michetti@cmcc.it (M. Michetti), enrico.scoccimarro@ingv.it (E. Scoccimarro), silviogualdi@ingv.it (S. Gualdi).

http://dx.doi.org/10.1016/j.scitotenv.2016.07.008

River discharge
Water resources

in the recent decades, but using different data. In addition, we found that the percentage of global area covered by heat wave exceeding a given magnitude has increased almost three times, in the last decades, with respect to that measured in the early 20th century. Finally, we discuss the specific implications of the heat waves on the river runoff generated in the Alps, for which comparatively long datasets exist, affecting the water quality and availability in a significant portion of the European region in summer.

1. Introduction

Heat waves are periods of abnormally hot weather. While the definition may vary across different studies, a wide consensus exists on the implications of the strongest events on, agriculture and land ecosystems (Ciais et al., 2005), wildfires and air pollution (Vautard et al., 2005), human comfort and mortality (WHO, 2004, 2010), and power shortages (Fink et al., 2004), amongst others.

Whether heat waves have increased in frequency, duration, and/or amplitude is a much-debated issue in climate change science. Given the limited data availability on a daily time scale, most studies of heat waves are based on data since 1950. On a global scale, there is a medium level of confidence that they have increased in frequency and/or duration (IPCC, 2013). It is likely that the frequency of heat waves has increased in large parts of Europe (Perkins et al., 2012; Della-Marta et al., 2007a). This is also connected to a drying trend in the Mediterranean (Zampieri et al., 2009; Wang et al., 2011), Asia (Perkins et al., 2012; Rahimzadeh et al., 2009; Ding et al., 2010), and Australia (Perkins et al., 2012; Perkins and Alexander, 2012; Tryhorn and Risbey, 2006). A general increase is also found, with less confidence, in Northern and Central America (Kunkel et al., 2008; Peterson et al., 2008; Perkins et al., 2012). However, the overall longer-term trend is negative in the U.S. if the so-called "Dust Bowl" that occurred in the 1930s is taken into account (Peterson et al., 2013). South America, Africa and Asia suffer from a lack of data. Nevertheless, in South America there exist more evidence on increases rather than on decreases (Skansi et al., 2013) and medium confidence of an increase in Northern Africa and the Middle East (Perkins et al., 2012; New et al., 2006) and in South Africa (Kruger and Sekele, 2013). It is very likely that heat waves will occur with a higher frequency, intensity and duration in the future, if there is an increasing concentration of greenhouse gases (IPCC, 2013; Russo et al., 2014).

Future trends in heat waves may also influence the supply of water. Runoff production and river discharge is expected to be anti-correlated with anomalous hot weather because of a variety of reasons and feedbacks processes. In fact, heat waves cause an increase of evapo-transpiration that reduces soil moisture, and soil moisture deficit itself can act as an amplifier of heat waves amplitude (see e.g. Seneviratne et al., 2010; van den Hurk et al., 2011). Moreover, in several regions as Europe and the Mediterranean - where the final part of this study is focused on - soil dryness can represent a precursor of heat waves in the summer season (Vautard et al., 2007; Zampieri et al., 2009), while circulation anomalies producing meteorological and soil dryness can be simply the same connected to hot weather (Della-Marta et al., 2007b; Lionello, 2012).

The combined surface temperature warming and the reduction in water availability showed the vulnerability of the energy sector in Europe and around the world (van Vliet et al., 2013; Scanlon et al., 2013; Koch and Vogele, 2009). Heat waves may physically damage electricity infrastructures (Depietri et al., 2012), causing problems for both energy generation and transmission (Matzarakis and Nastos, 2011), and thereby affecting energy supply. This may result from both low water availability and quality (van Vliet et al., 2013). The increase in consumers' demand combined to a shortage in supply due to the warm and dry summers of 2003, 2006, 2009 has led to higher variability of energy prices and to an increase in electricity prices in several European countries (van Vliet et al., 2013). On a similar ground, heat waves lead to an increase in water consumption (Rinaudo et al., 2012) and to a decrease in water quality (Wetz and Yoskowitz, 2013). Indeed, peak demand associated with energy consumption during hot summers has become a problem in many developing and in some developed countries as well (Strengers, 2012). For example, the effects of the 2010 Russian heat wave extended as far as the Red Sea region. Temperatures reached 52.0 °C in Jeddah (WMO, 2011), causing unprecedented demand for electricity for air conditioning and which led to blackouts in the whole Saudi kingdom (Gulf News, June 22, 2010, 'Heatwave in Middle East no cause for panic').

Recently, a new Heat Wave Magnitude Index daily (HWMId) has been introduced (Russo et al., 2015) in order to capture both the intensity and duration of a heat wave. The HWMId sums excess temperatures beyond a certain normalized threshold and merges durations and temperature anomalies of intense heat wave events into a single number. The HWMId is the improvement of the previous Heat Wave Magnitude Index (i.e., HWMI, Russo et al., 2014), overcoming the HWMI limitations in assigning magnitude to very high temperatures in a changing climate (for further detail see Russo et al., 2014, 2015). The HWMId is the most widely applicable index currently available and allows heat waves to be compared across different regions and time periods.

In this study, we compute the HWMId on the reanalyses of the 20th Century, recently produced by the National Oceanic and Atmospheric Administration (NOAA, Compo et al., 2011, 2015) and the European Centre for Medium-Range Weather Forecasts (ECMWF, see link in References). The reanalyses are created through an assimilation procedure that integrates the information from the observations into numerical models. The models are used to "fill the gaps" in the observations, leading to a comprehensive representation of the atmospheric circulation and the land surface variables, including those that are not measured but are included in the model formulations. In this way, the weather of the past can be reconstructed globally, including the regions with scarce data coverage. In general, there is an unresolved issue about trend computation on reanalyzed data because of the quality and the coverage of the observed data change in time, affecting the homogeneity of the products. As explained in the data and methods section, the 20th Century Reanalyses adopted here limit this problem as much as possible. Thus, they are the most homogeneous representation of the atmospheric circulation and land surface variability currently available at the global scale and over the long time-scales we are addressing. The 20th Century Reanalysis produced by NOAA, for instance, has been successfully adopted for regional long-term studies of decadal climate variability (Zampieri et al., 2013) and long-term trends (Zampieri et al., 2015, see also Parker, 2011for a validation of the recent trend and of the daily temperatures of the 20CR-2 against observations). While our results are consistent with recent studies analyzing heat waves occurred after 1950, it must be noted that a strict validation of the daily data is impossible for the earlier period at the global level.

However, given the importance of heat waves for ecosystems, economies and societies, it is still interesting and useful to produce a global assessment of the larger events occurred in the entire century, especially in the regions characterized by scarce knowledge of the past climate, which are often the most vulnerable to the impacts of climate change. Our results are comparable with local records, documentary sources and non-peer reviewed literature for the specific regions of interest. In particular, we also conduct a specific validation of the heat waves

variability in the Alps, often referred as the "water towers of Europe" (Beniston et al., 2011), in order to assess the correlation between the climate variability connected to heat waves occurrence and the river discharge originating there. This effort can potentially reduce the gaps between the understanding of the effects of climate variability on water resources and the need for a development of a water-related decision-making framework in that region (Ludwig and Roson, 2016).

2. Data and methods

In order to produce a general assessment analysis of heat waves on a global scale and over a long period, we adopt the Heat Wave Magnitude Index daily (HWMId, Russo et al., 2015). The HWMId is defined as the maximum magnitude of the heat waves in a year, where a heat wave is a period of at least 3 consecutive days with maximum temperature exceeding the daily threshold for the reference period (1981–2010). The threshold is defined as the 90th percentile of daily maxima temperature, centered on a 31 day window. The HWMId is the sum of the magnitude of the consecutive days composing a heat wave, with daily magnitude calculated by means of the magnitude daily function (Md) as defined in Russo et al., 2015. The HWMId calculation in this study has been done by using the "HWMId" R function, recently published in the R package called extRemes (Gilleland and Katz, 2011).

We compute the HWMId on maximum daily temperature data from long-term atmospheric reanalyses, forced by prescribed SST and Sea ice and letting land surface processes free to evolve: the 20th Century Reanalysis version 2 (20CR-2, Compo et al., 2011), produced by National Oceanic and Atmospheric Administration (NOAA) and available from 1871 to 2012 on a Gaussian T62 grid (i.e. 192×94 points, corresponding to the centers of regularly spaced cells in longitude and latitude); the newer version of NOAA reanalysis (version 2c, 20CR-2c, Compo et al., 2015), produced in collaboration with the University of Colorado Cooperative Institute for Research in Environmental Sciences (CIRES) and extended back in time to 1851. 20CR-2c uses the same model as version 2 with new sea ice boundary conditions from the COBE-SST2 (Hirahara et al., 2014), new pentad Simple Ocean Data Assimilation with sparse input (SODAsi.2, Giese et al., 2015) sea surface temperature fields, and additional observations from ISPD version 3.2.9 (Cram et al., 2015); ERA-20C, produced by the European Center for Medium Weather Forecasts (ECMWF) and available from 1900 to 2010 at a horizontal resolution of about 125 km (spectral truncation T159). Given the possibility of downloading this reanalysis at different resolutions, we have chosen the 1.5 degrees product (240×120 points), ensuring a better consistency with 20CR-2 and 20CR-2c. The observations assimilated in ERA-20C include surface and mean sea level pressures from ISPDv3.2.6 and ICOADSv2.5.1, and surface marine winds from ICOADSv2.5.1 (Woodruff et al., 2011).

These reanalyses are produced by adopting a minimal number of observations with respect to the earlier reanalyses focusing on recent decades (which tend to use all available data, disregarding homogeneity issues). Namely, the considered observations consist of sea surface temperature (SST) and sea ice distribution (and sea wind, in ERA-20C), atmospheric CO_2 concentrations, solar and volcanic forcings (as boundary conditions) and surface pressure (as assimilated data). Land surface temperature is free to evolve. Reanalyses uncertainty depends on the quality of the atmospheric model and data, on the accuracy of the model's response to the large-scale forcings and to the sparse assimilated surface pressure data and on the intrinsic predictability of the heat waves events from these forcings. Also, the need to parameterize the details of the land-surface processes and their interactions with the atmosphere further amplifies the uncertainty associated to the Reanalyses' results. Thus, there is no guarantee that all heat waves we are looking for are correctly reproduced in terms of magnitude and spatial coverage. This motivated us to compare these reanalyses among each other and to produce an integrated dataset that maximized the skill in diagnosing the heat waves more reliably.

All the reanalyses considered here are actually comprised of an ensemble of model simulations starting from perturbed initial conditions in order to account for the variability associated with the models' response. We show the HWMId computed on the ensemble means, which are the freely available products. Moreover, we provide a single estimate of heat waves variability, integrating the information from all the datasets. A difficulty rises from the fact that the reanalyses are not completely independent, especially the NOAA ones. Therefore, some sort of weighting is necessary to obtain a final unbiased averaged estimate. We simply average together the HWMId computed on NOAA reanalysis, restricting our analysis to the two most independent products - ECMWF reanalysis itself, and the average of NOAA's reanalyses - and we average these two together to obtain the final weighted average estimate, with the least loss of available information.

We validate the three long-term reanalysis and their weighted average for the present climate using the HWMId computed on the more conventional reanalyses, which assimilate all possible observations in order to maximize the accuracy of the product. These are, namely, NCEP-2 (Kanamitsu et al., 2002) and ERA-Interim (ERA-Int, Dee et al., 2011), defined in the period covered by satellites, from 1979 to present, and NCEP-1 (Kalnay et al., 1996) and ERA-40 (Uppala et al., 2005), covering also earlier periods (from 1948 to present and from end of 1957 to 2002, respectively). Fig. 1 show the spatial distribution of the skills of the longer-term reanalysis computed with respect to the shorter-terms one. The panels show the frequency for which the events are correctly captured. For each year, an event is considered as correctly captured if the HWMId predicted by the longer-term reanalysis is at least half of that computed on the shorter-term reanalyses and no more than double. This includes the true negatives, i.e. the years when both the longer-term and the shorter-term reanalysis diagnose no heat waves (HWMId $= 0$), allowing a small confidence interval (HWMId $= 1$). This criterion is consistent with the 'percent correct', used to measure the skill of precipitation simulations in meteorology.

All Reanalyses show some skill (see Fig. 1). The skills vary depending on the dataset and in space. The 20CR-2 is correctly capturing the HWMId most of the years in most of the regions, especially compared with the more recent reanalyses (NCEP-2 and ERA-Int), with the notable exception of the North American plains and Argentina. The recent update of 20CR-2c resulted in an overall degradation of this result, especially in the tropics and Northeast Asia. ERA-20C skill is approximately between those of the NCEP Reanalyses. It is poorer than them especially in Brazil and India. The weighted average shows the best skill in almost all areas.

We compute the decadal maxima HWMId time-series from the individual reanalyses following the IPCC regionalization, as defined in the Special Report on Managing the Risks of Extreme (SREX, Seneviratne et al., 2012). For the weighted average, we plot the spatial distribution of the decadal maxima, together with a quantification of the accuracy in terms of the level of agreement among the individual datasets. To measure this, we define a signal-to-noise ratio of the detected heat waves in terms of the ratio between the weighted mean HWMId and the absolute difference between the NOAA averaged HWMId and ECMWF HWMId. We set an arbitrary threshold at 1, meaning that we highlight a certain heat wave obtained from the weighting average procedure if a heat wave of at least half magnitude is present either in ECMWF or in the combination of the NOAA reanalyses.

We provide a cross-comparison of the HWMId time series with the river discharge originated over the Alps, using data provided by the Global Runoff Data Center (GRDC, see link in References). With this analysis, we provide a measure of the consistency of heat waves and river discharge time-series, and a certain degree of validation of the inter-annual variability and long-term trend of both datasets before the period covered by the recent Reanalyses.

Fig. 2 shows the spatial distribution of the gauge stations and the corresponding contributing basins in the Alpine region. The climatic characteristics of this study area are discussed by Zampieri et al.

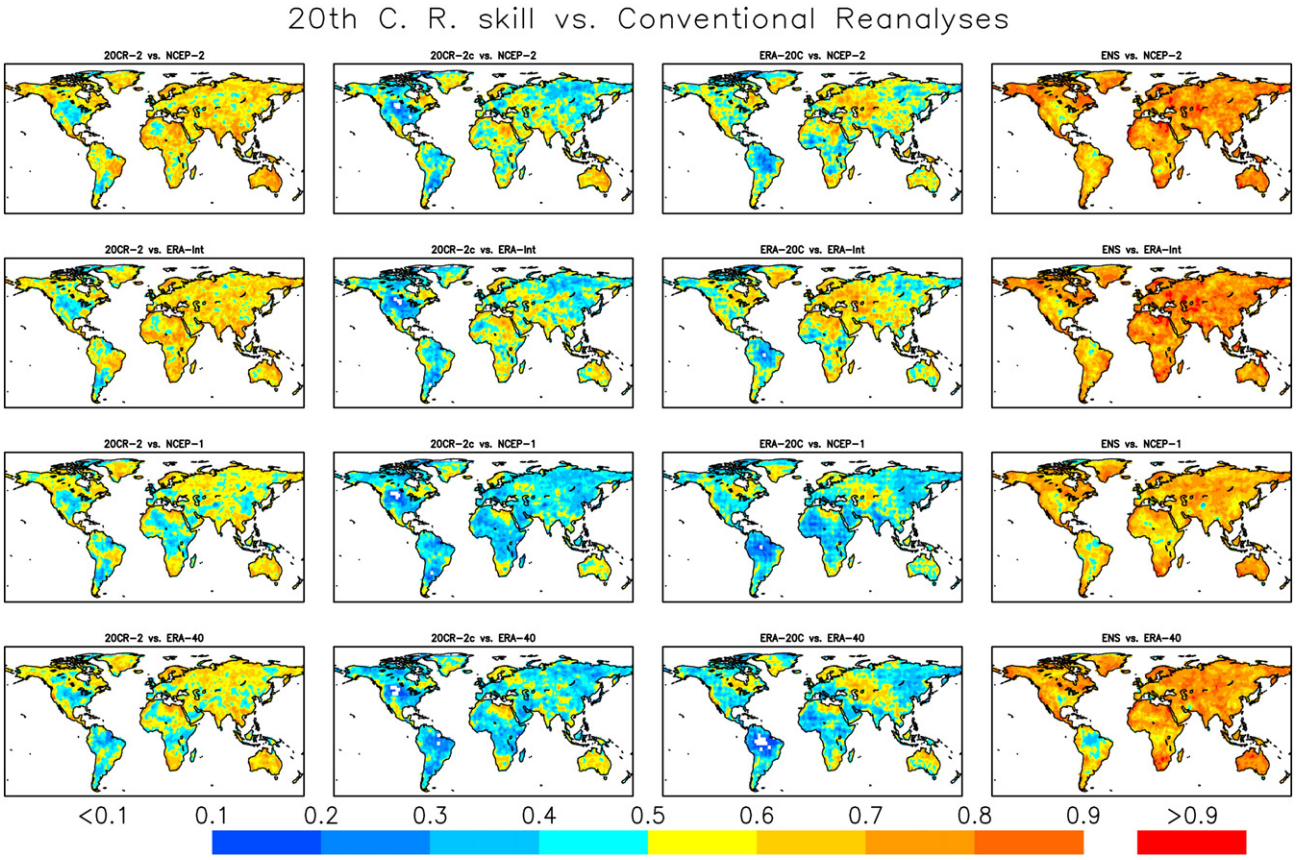

Fig. 1. Skills of the NOAA 20th Century Reanalysis version 2 (20CR-2), of the 20th Century Reanalysis version 2c (20CR-2c), of the ERA-20C, produced by ECMWF, and their weighted average in reproducing the annual HWMId values computed on "Conventional" Reanalysis: NCEP-2, over period 1979–2010, ERA Interim (ERA-Int), over period 1979–2010, NCEP-1, over period 1948–2010, and ERA-40, over period 1958–2002. The panels show the frequency of years when the heat waves are correctly captured (within a certain confidence range), including the true negatives (see Data and methods for explanations).

(2015), for each basin. Most of the precipitation is located over the orography, with seasonal variations that depend on the location. The seasonal precipitation cycle varies from a continental one in the northern flank of the Alps, characterized by a maximum in summer, to a more reminiscent of the 'Mediterranean like' climate, characterized by a summer minimum, in the southern flank. In fact, in the southern flank, precipitation shows two peaks in the intermediate season. The Alpine and surrounding regions can be subject to heat stress in summer.

For the river discharge originated over the Alps, in order to have a good compromise between the spatial coverage of the signal footprint and length of the records, we sum up the contributions of the four major rivers. Namely, they are the Rhine, the Danube, the Rhone and the Po rivers. The resulting time-series integrating the four river discharges is defined from 1921 to 2007. Unfortunately, data provided by GRDC do not cover the last years for the Rhone and the Danube rivers. In order to account for a lag between the heat waves occurring in summer and the river discharge recoded at the gauge stations, we related the HWMId maximum computed over the Alpine region to the total discharge recorded in August (see Zampieri et al., 2015 for a discussion of this topic and a description of the river discharge data provided by GRDC). We compare the river discharge data with the HWMId time-series computed over an area covering the basins where the rivers runoff is generated. More precisely, we consider the maximum HWMId between 5E to 15E and 44E to 49N (area depicted in Fig. 2). Given the relatively low resolution of the reanalyses and the spatial coherence of the heat waves, the results are not sensitive to small changes in the definition of the area where the index is computed. In order to show the consistency of the two datasets in terms of inter annual variability and long-term trends, we simply discuss the correlations of the annual HWMId and August discharge values, also showing the time-series of the decadal means.

3. Results and discussion

Fig. 3 shows the HWMId spatial maximum computed for each IPCC-SREX region and for each decade of the 20th Century Reanalyses (20CR-2, 20CR-2c and ERA-20C). The overall magnitude of heat waves varies with the region, reflecting the different climates and different climatic variability (note that the scales of the y-axis vary with the region). A first visual impression suggests that the nature of these events is so intermittent that it strongly limits the validity of linear trends computation, even with such long datasets. For instance, a single large heat wave at the beginning or the end of the records is sufficient to dominate the linear trend computed in most of the regions. Moreover, the effects of natural climate variability may be more significant than those related to global warming at the regional level. In fact, the trends would change significantly if computed from 1950 or earlier, in most regions. For these reasons, we do not show the results of linear HWMId trends.

The level of agreement among the datasets can be roughly assessed by comparing the time-series plotted in Fig. 3. In general, the two reanalyses from NOAA tend to be more similar to each other than to the ECMWF one, as anticipated. The plotted maxima computed on the individual datasets could be located in different portions of the regional domains and could have happen in different years of the decades. The comparison with the weighted average can be used to better quantify this uncertainty. Low HWMId values in the weighted average compared to the individual datasets indicate poor agreement in the location and/or in the timing of the diagnosed heat waves. The specific year

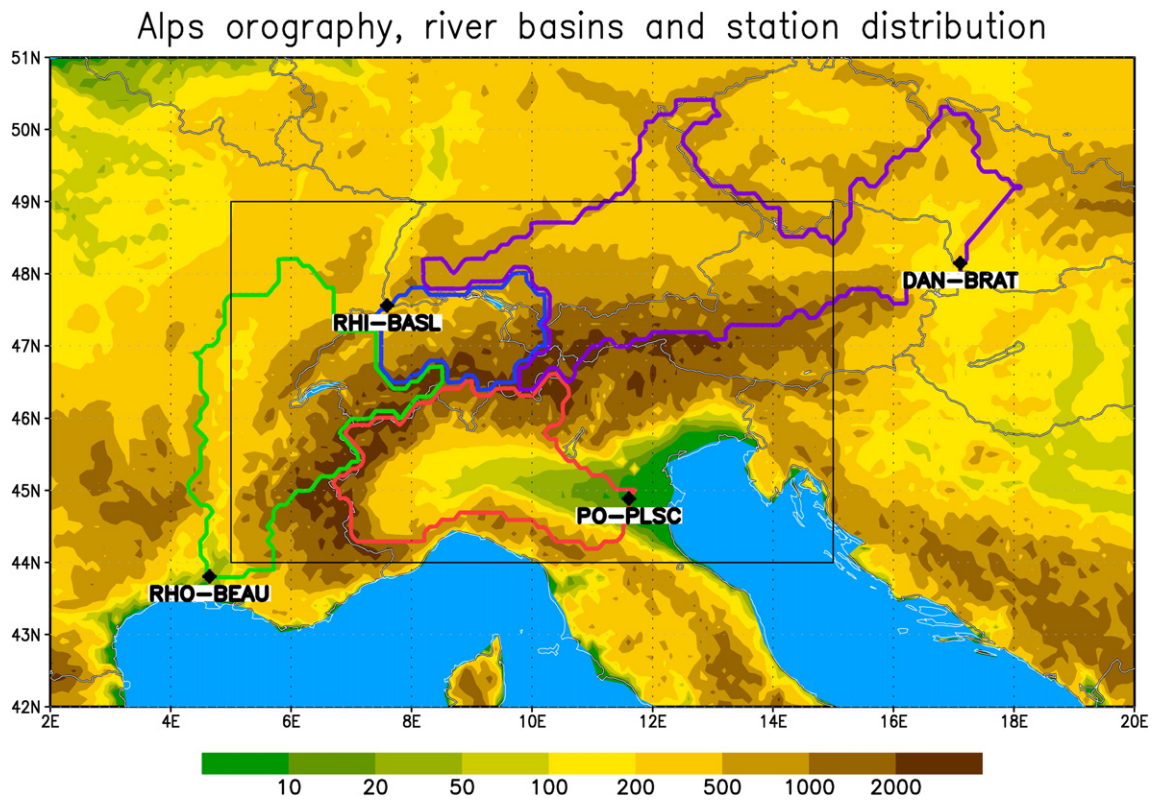

Fig. 2. Distribution of the four stations (black diamonds) representative of the four major Alpine rivers and the respective contributing basins: the Rhine river in Basel (RHI-BASL, 7.59E-47.55N, blue contour), the Danube river in Bratislava (DAN-BRAT, 17.11E-48.14N, violet contour), the Rhone river in Beaucaire (RHO-BEAU, 4.64E-43.81N, green contour) and the Po river in Pontelagoscuro (PO-PLSC, 11.60E-44.89N, red contour). The filled contours depict the orography height (in m). The inner black box depicts the area where the HWMId displayed in Fig. 5 is computed. This area includes 17 land points of the NCEP Reanalyses (20CR-2 and 20CR-2c) and 20 land points of the ECMWF one (ERA-20C).

responsible for the decadal regional maxima can be deduced by comparison with Fig. S1, where we also include the results of the weighted average in order to provide a more reliable result, and to quantify the spatial uncertainty of the individual Reanalyses.

In Fig. 4, we plot the spatial distribution of the decadal maxima of the weighted averaged HWMId computed since 1901, where all datasets overlap. We mask the regions where the detected signals correspond to a low level of agreement between the datasets, as the consistency condition is not satisfied (signal-to-noise ratio < 1), for each year. This is a more stringent condition with respect to the simple comparison of the regional maxima of the individual datasets shown in Fig. 3.

We now discuss more explicitly some of the most significant heat waves that occurred in the same region and decade. For instance, in the U.S., we notice that the largest value, found in the 1930s, is actually a superimposition of several heat waves that occurred in most of the years of that decade, but with different intensities and variable spatial distribution. The largest HWMId and spatial extensions are found in 1931, 1934, 1936 and 1937. All these were comparable in magnitude and spatial extent to the most extreme heat wave in our historical record that occurred in Russia in 2010. Unfortunately, they are only partially reproduced by ECMWF reanalysis. Similar, less intense events happened in the decades before and after with different spatial distributions. It is worth noting that this region is characterized by comparatively low skill in the Reanalyses (see Fig. 1). The 1980 heat wave in the U.S. is less intense than the events happened in the 1930s in the same region. A detail to note here is that the decade is defined from “year 1” to “year 10”, so that the 1970s decadal maxima are computed from 1971 to 1980. Often, the largest events that occurred in South American countries at about an Equatorial latitude took place synchronously with the events recorded in North America, while the events recorded in the Central and Southern part of South America seemed to happen independently. We note a noteworthy heat wave occurred in 1971 in La Plata Basin (Argentina), which is reproduced by all datasets despite the comparatively low skill in that region (see Fig. 1). This event is not even reproduce by ERA-40 or NCEP-1 (not shown), but we found a record of it in documentary sources (Zamboni et al., in preparation). In this region, the large event displayed in the 1980s is produced only by NOAA reanalyses in 1985, but not by ECMWF. They all show an extreme heat wave in the same year on the southern border of the continent.

A better data agreement has been found over Europe, especially since the 1950s (see also Fig. 1). In this case, the recorded heat waves show quite similar extension and magnitude compared with Russo et al. (2015) study, which is based on observed data. They include the heat waves found in 1954 in Russia, 1969 in Norway, 1972 in Finland and the Kola Peninsula, 1976 in UK, 1994 in Germany, 2003 in Western EU, 2006 in Central EU, 2007 in the Balkan Peninsula and 2010 in Russia. Interesting earlier large heat waves are found in Europe before the 1950s. Several events occurred in the first part of the 20th Century in the Baltic region (notably, the one in 1914), Russia and Turkey. The first significant event affecting Central Europe is found in 1938 in the NOAA reanalysis, while a severe heat wave over Russia emerges in all of the considered reanalyses, during the same year. The maximum displayed in the 1940s in Fig. 4 is due to an event that occurred in 1946 in all of the datasets. We also identified an interesting heat wave in Ireland in 1955. This was actually already documented. In fact, it was ranked as one of the sunniest summers ever recorded by the Observatory of Armagh in the last 100 years (McNeill, see link in References).

The majority of heat waves we recorded happened independently in different regions. Nevertheless, the 2010 Russian event was actually of a “global” nature, as it simultaneously affected regions other than Russia, often spatially interconnected. These included Turkey, the Red Sea region, part of the Sahel, Southern Greenland, Southern U.S., South

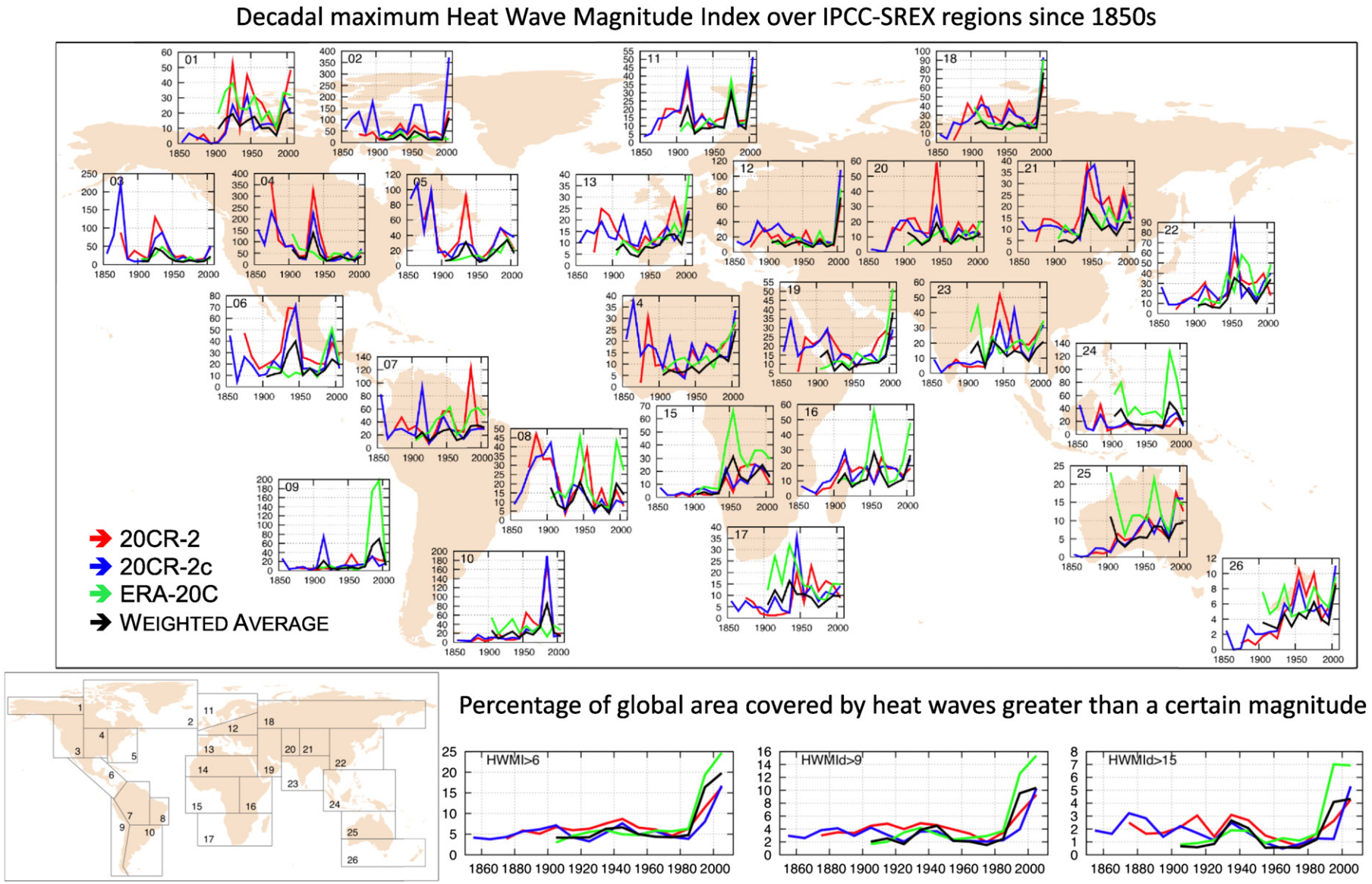

Fig. 3. Decadal maximum Heat Wave Magnitude Index (HWMId) over IPCC regions, as defined in the Special Report on Managing the Risks of Extreme (SREX, Seneviratne et al., 2012). The time-series show the results computed on the NOAA 20th Century Reanalysis version 2 (20CR-2), in red, on the 20th Century Reanalysis version 2c (20CR-2c), in blue, for the ERA-20C, produced by ECMWF, in green, and their weighted average (see text for explanations), in black Note that the scales of the y-axis vary with the region. The bottom panels show the decadal maxima of global percentage of areas covered by heat waves greater with magnitude > 6, 9 and 15, computed from the same datasets.

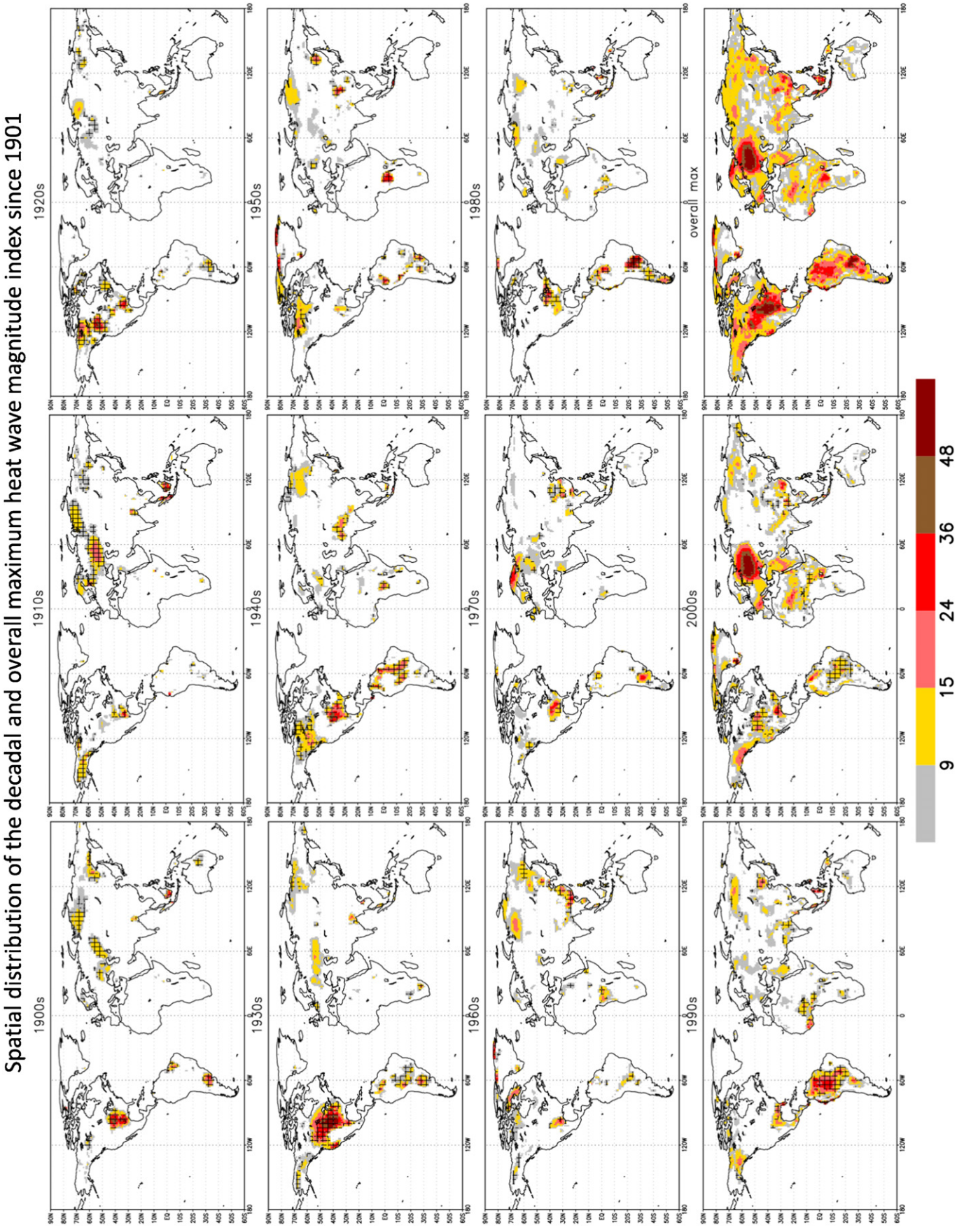
Spatial distribution of the decadal and overall maximum heat wave magnitude index since 1901
1900s
1910s
1920s
1930s
1940s
1950s
1960s
1970s
1980s
1990s
2000s
overall max
9
15
24
36
48

American countries along the Equator, Peru, and Indonesia. Also in 2003, different regions were affected by synchronous heat waves, but to a lesser extent than in 2010. In 2003 Western Europe, Eastern China, Bangladesh, the Western US, Southern Canada and Colombia were affected by extreme heat waves. It is worth noting that in 1998 we found extreme heat waves in the Southern US, Florida, Central America, the Northern part of South America, West Africa towards the Gulf of Guinea, the Central part of the Arabian Peninsula, the Indonesian Peninsula and Borneo. These heat waves are poorly discussed in the literature. Fewer and more limited synchronous heat waves are present in the earlier records.

Africa was affected by several heat waves in the past, but there is limited agreement among datasets with the notable exception of Central Western Africa in 1968, Central Eastern Africa in 2005, and the 1998 and 2010 "global" events. All datasets agree that a severe heat wave happened in Egypt in 1965. Similarly, a severe HW affected the Middle Eastern countries facing the Eastern Mediterranean coast in 1987. In 2001, an extreme heat wave struck Iraq and northern Saudi Arabia; this is not clearly visible in Fig. 4 because it is merged with the 2010 event.

Central and Northern Asia are affected by a large number of heat waves of severe and extreme magnitude in all decades. Notable and recurrent events, often reported by all datasets, are located in Central Siberia, as in 1953, for instance and in southwestern Russia, north of the Black and the Caspian Seas. Several heat waves affected the Himalayan Chain in the 1940s, preceded by an extreme heat wave in Bangladesh in 1935. These are found in all Reanalyses, as well as an extreme heat wave in Central China in 1957.

Australia, which is one of the warmest and most arid regions of the World, displays low HWMId values with respect to the local climate variability. Here, HWMId increased almost monotonically since the beginning of the records. The largest heat waves are found in recent decades (and in all datasets), affecting the northwestern part of the continent in 1991 and the southeastern part in 2009.

The time-series global percentage of land areas covered by heat waves with HWMId larger than certain thresholds (Fig. 3) provide the clearest evidence that something has changed in the last two decades. Earlier, the percentage of areas covered by heat waves was actually almost constant. The widespread synchronous heat waves that occurred in 1998, 2003 and 2010 are responsible for the discontinuity that we observe in all these time-series. The percentage of areas affected by heat waves increases about three times for HWMId larger than 6 and 9 and about twice for HWMId larger than 15 during the last two decades in the NOAA Reanalysis. We found an even larger increase in the ECMWF dataset. The weighted average shows consistent results. This is most probably the most striking outcome of our global heat waves assessment.

Fig. 5 shows the time-series of the HMWId computed over Alps for the three reanalysis, their weighted mean, and the total discharge contributing to the Rhine, Danube, Rhone and Po river. The multiple reasons discussed in the introduction are indeed responsible for a high level of consistency between heat waves occurrence and negative river discharge anomaly, as expected. From the annual values, it is possible to infer a significant (anti)correlation of the data. The values we computed are shown in Table 1. Linear correlations are −0.72 for the weighted mean index, −0.62 for 20CR-2, −0.56 for 20CR-2c and −0.64 for ERA-20C if computed until 1960, when the majority of the dams and hydraulic structures where built (Zampieri et al., 2015). Lower correlations, around −0.5, characterize the full time-series (see the second row of Table 1). Visual inspection of the decadal means also show a high level of consistency, especially regarding the warm-dry event in the 1950s and the trend characterizing the following decades. The major mismatch is in the last decade. 20CR-2 and 20CR-2c show a relatively warm period over the Alps at the end of the 19th Century.

4. Conclusions

We have provided an assessment of decadal climate variability of heat waves, based on the most homogeneous climate reconstruction datasets currently available over the longest period and on a daily basis, using a new non-parametric estimator: the Heat Wave Magnitude Index (HWMId, Russo et al., 2015).

In the decade 2001–2010 the percentage of global area covered by heat wave with a given magnitude (e.g. HWMId ≥ 6, HWMId ≥ 9) has increased at least three times with respect to that measured in the early 20th century.

Climate variability and the intermittent nature of these regional scale extreme events make simple linear trend estimation meaningless, even if the computation is performed over the longest period of time for which data is available (1850). A notable exception is in Australia, especially the southern part, for which all datasets show a positive HWMId trend that is probably related to the general warming of that region. Our study is consistent with other assessments based on different data and documentary sources for past events. Moreover, we discovered heat waves that have been never discussed, especially in regions with limited data availability. We provide readers with additional information for specific areas of interest following the IPCC regionalization, as defined in the Special Report on Managing the Risks of Extreme.

We diagnosed the emergence of widespread synchronous heat waves at the end of the 1990s and in the 2000s (i.e. in 1998, 2003 and 2010). This emerging phenomenology is responsible for the dramatical increase of the global area affected by extreme heat waves that occurred over the last two decades, while the earlier period showed little or no variation in this sense.

The physical reasons and the processes involved in generating such events needs to be further explored and explained in order to provide a deeper understanding of the present climate and to offer a solid basis for the interpretation of future climate projections. Nevertheless, our study offers an immediate understanding of past heat waves' long-term variability which might be useful for the interpretation of the relative magnitude of current and future heat waves for adaptation planning.

Heat waves occurrence and magnitude is significantly correlated to negative anomalies of river discharge originated over the Alps. This poses legitimate concerns on the possible effects of a potential increases of heat wave magnitudes in the future climate, which we already noted in the last decades. Dams and hydraulic structure partially decouple the river discharge variability from the inter-annual climate variability, and may be used as a partial measure for counteracting the effects of climate change on water availability for a large portion of Europe. On the other hand, short-term adaptation strategies should be envisaged in the energy sector, to prevent undesired and distorted distributional and allocative socio-economic effects due to changes in water availability, energy supply, and therefore energy prices causing misallocation of scarce resources. In fact, the existence of a negative correlation between heat waves occurrence and river discharge that we diagnosed in summer is likely to exacerbate an already existing problem of water scarcity with important implications for health and the economy (Ludwig et al., 2011).

Indeed, the European energy sector, in addition to being directly sensitive to warm conditions, it is highly dependent on water availability (43% of total surface water withdrawal, according to EUREAU, 2009),

Fig. 4. Decadal maximum of weighted mean HWMId computed from the three datasets (see text for explanations). Each decade is defined from year 1 to year 10 (i.e. 2000s indicates the maximum HWMId from 2001 to 2010). Values smaller than 2 (normal heat waves) are masked. Shaded areas indicate regions of scarce agreement among the datasets and low reliability of the displayed value (see text for explanations). The bottom-right panel shows the overall maximum computed since 1901, where all datasets overlap.

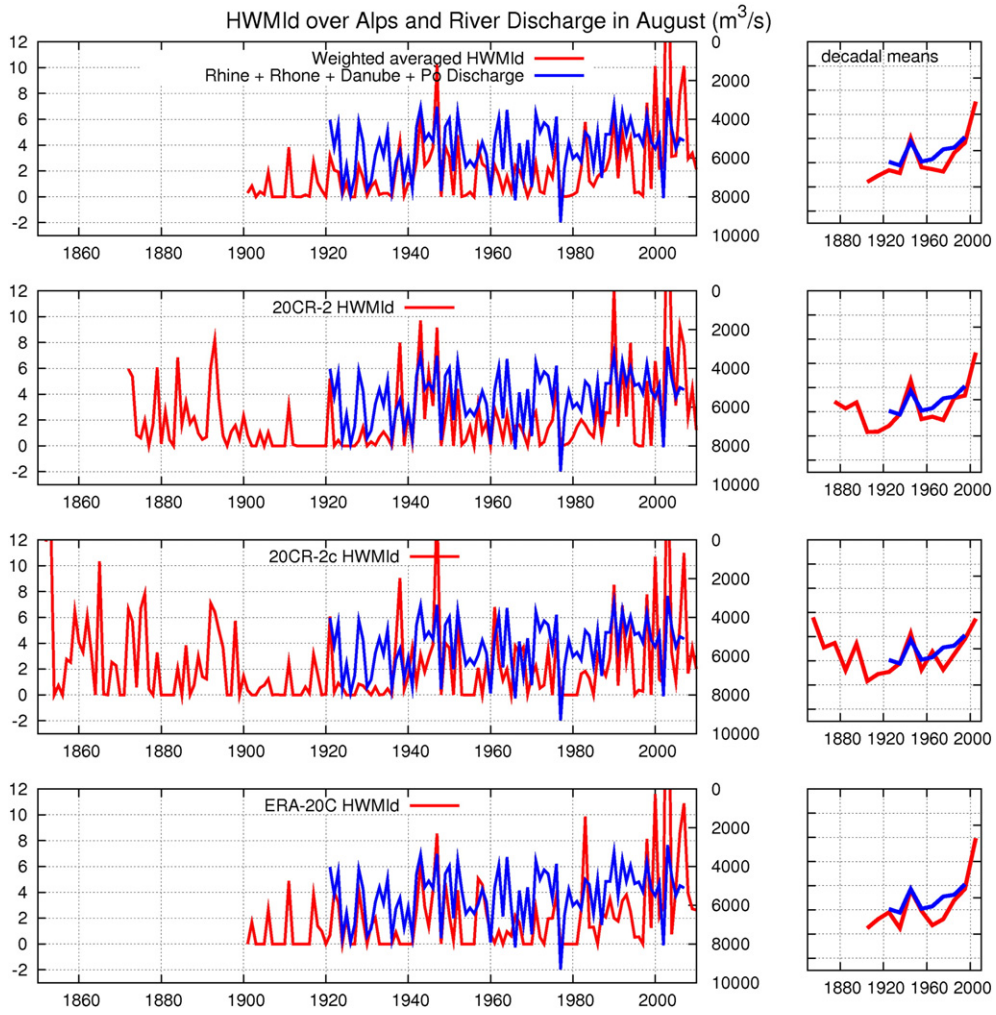

Fig. 5. Time series of HWMId computed over the area from 5E to 15E and from 44N to 49N, covering approximately the basins of the Rhine, Rhone, Danube and Po rivers relative to the gauge station located at Basel, Beaucaire, Bratislava and Pontelagoscuro, respectively (in red, left axes), and the sum of the river discharge (in blue, right axes, in cubic meters per second, see Zampieri et al., 2015 for a description of the river basins, stations and data). Panels from top to bottom show the comparison of the data for the 20th Century Reanalysis version 2 (20CR-2), for the 20th Century Reanalysis version 2c (20CR-2c), for the ECMWF reanalysis (ERA-20C), and for the weighted mean of them. Left panels show the annual values. Right panels show the decadal mean time-series plotted on the same axes of the left panels.

and quality. Van Vliet et al. (2013) anticipate a strong decline in projected river flows for central, southern, and southeastern Europe during 2031–2060 relative to 1971–2000 period. This reduction is mainly concentrated in the summer season, over the Alps, where it may pose some concern on water regulation to guaranty the minimum ecological flow (Majone et al., 2016). Therefore, we expect higher competition in the use of water in order to respond, simultaneously, to the population's need of drinking water, to the demand coming from different market sectors (e.g., agriculture, energy etc.) and to the ecosystems' needs.

Supplementary data to this article can be found online at http://dx.doi.org/10.1016/j.scitotenv.2016.07.008.

Table 1
Linear correlations between the HWMI and river discharge computed over the Alps (5E–15E, 44N–49N) and shown in Fig. 5. The first row shows the results of the correlations computed till 1960, when most of the hydraulic structures were built (Zampieri et al., 2015). The second row shows the results computed over the entire time-series.

Period	Weighted mean	20CR-2	20CR-2c	ERA-20C
1921–1960	−0.72	−0.62	−0.56	−0.64
1921–2007	−0.48	−0.54	−0.46	−0.39

Acknowledgements

This work was supported by the Italian Ministry of Environment, Land and Sea under the GEMINA and NEXTDATA projects and by the H2020 CRESCENDO project (Grant No. 641816). We express our gratitude to Savino Sasso for keeping our computers in the best possible working condition and for his scientific interest and intuition while commenting the results of this study.

References

Beniston, M., Stoffel, M., Hill, M., 2011. Impacts of climatic change on water and natural hazards in the Alps: can current water governance cope with future challenges? Examples from the European "ACQWA" project. Environ. Sci. Pol. 14, 734–743.

Ciais, P., Reichstein, M., Viovy, N., Granier, A., Ogée, J., Allard, V., Aubinet, M., Buchmann, N., Bernhofer, C., Carrara, A., Chevallier, F., De Noblet, N., Friend, A.D., Friedlingstein, P., Grünwald, T., Heinesch, B., Keronen, P., Knohl, A., Krinner, G., Loustau, D., Manca, G., Matteucci, G., Miglietta, F., Ourcival, J.M., Papale, D., Pilegaard, K., Rambal, S., Seufert, G., Soussana, J.F., Sanz, M.J., Schulze, E.D., Vesala, T., Valentini, R., 2005. Europe-wide reduction in the primary productivity caused by the heat and drought in 2003 (Nature). 437, 529–533.

Compo, G.P., Whitaker, J.S., Sardeshmukh, P.D., Matsui, N., Allan, R.J., Yin, X., Gleason, B.E., Vose, R.S., Rutledge, G., Bessemoulin, P., Brönnimann, S., Brunet, M., Crouthamel, R.I., Grant, A.N., Groisman, P.Y., Jones, P.D., Kruk, M., Kruger, A.C., Marshall, G.J., Maugeri, M., Mok, H.Y., Nordli, Ø., Ross, T.F., Trigo, R.M., Wang, X.L., Woodruff, S.D., Worley, S.J., 2011. The twentieth century reanalysis project. Quarterly J. Roy. Meteorol. Soc. 137, 1–28.

Compo, G.P., et al., 2015. NOAA/CIRES Twentieth Century Global Reanalysis Version 2c. Research Data Archive at the National Center for Atmospheric Research, Computational and Information Systems Laboratory. http://dx.doi.org/10.5065/D6N877TW (updated yearly).
Cram, T.A., Compo, G.P., Yin, X., Allan, R.J., McColl, C., Vose, R.S., Whitaker, J.S., Matsui, N., Ashcroft, L., Auchmann, R., Bessemoulin, P., Brandsma, T., Brohan, P., Brunet, M., Comeaux, J., Crouthamel, R., Gleason Jr., B.E., Groisman, P.Y., Hersbach, H., Jones, P.D., Jonsson, T., Jourdain, S., Kelly, G., Knapp, K.R., Kruger, A., Kubota, H., Lentini, G., Lorrey, A., Lott, N., Lubker, S.J., Luterbacher, J., Marshall, G.J., Maugeri, M., Mock, C.J., Mok, H.Y., Nordli, O., Rodwell, M.J., Ross, T.F., Schuster, D., Srnec, L., Valente, M.A., Vizi, Z., Wang, X.L., Westcott, N., Woollen, J.S., Worley, S.J., 2015. The International Surface Pressure Databank version 2. Geoscience Data J. 2, 31–46. http://dx.doi.org/10.1002/gdj3.25.
Dee, D.P., Uppala, S.M., Simmons, A.J., Berrisford, P., Poli, P., Kobayashi, S., Andrae, U., Balmaseda, M.A., Balsamo, G., Bauer, P., Bechtold, P., Beljaars, A.C.M., van de Berg, L., Bidlot, J., Bormann, N., Delsol, C., Dragani, R., Fuentes, M., Geer, A.J., Haimberger, L., Healy, S.B., Hersbach, H., Hólm, E.V., Isaksen, L., Kållberg, P., Köhler, M., Matricardi, M., McNally, A.P., Monge-Sanz, B.M., Morcrette, J.-J., Park, B.-K., Peubey, C., de Rosnay, P., Tavolato, C., Thépaut, J.-N., Vitart, F., 2011. The ERA-Interim reanalysis: configuration and performance of the data assimilation system. Q.J.R. Meteorol. Soc. 137, 553–597. http://dx.doi.org/10.1002/qj.828.
Della-Marta, P.M., Haylock, M.R., Luterbacher, J., Wanner, H., 2007a. Doubled length of western European summer heat waves since 1880. J. Geophys. Res. Atmos. 112, D15103.
Della-Marta, P.M., Luterbacher, J., Weissenfluh, H., Xoplaki, E., Brunet, M., Wanner, H., 2007b. Summer heat waves over western Europe 1880–2003, their relationship to large-scale forcings and predictability. Clim. Dyn. 29 (2–3), 251–275.
Depietri, Y., Renaud, F.G., Kallis, G., 2012. Heat waves and floods in urban areas: a policy-oriented review of ecosystem services. Sustain. Sci. 7 (1), 95e107.
Ding, T., Qian, W.H., Yan, Z.W., 2010. Changes in hot days and heat waves in China during 1961–2007. Int. J. Climatol. 30, 1452–1462.
ECMWF, European Center for Medium Range Weather Foracasts, 20 Century Reanalysis (E20): http://www.ecmwf.int/en/research/climate-reanalysis/era-20c.
EUREAU, 2009. Statistic Overview on Water and Wastewater in Europe 2008. European Federation of National Associations of Water and Wastewater Services, Brussels.
Fink, A.H., Bruecher, T., Leckebusch, G.C., Krueger, A., Pinto, J.G., Ulbrich, U., 2004. The 2003 European summer heatwaves and drought—synopstic diagnosis and impacts. Weather 59, 209–216.
Giese, B.S., Seidel, H.F., Compo, G.P., Sardeshmukh, P.D., 2015. An ensemble of historical ocean reanalyses with sparse observational input. J. Geophys. Res - Oceans (submitted). (SODAsi.2) http://www.esrl.noaa.gov/psd/data/gridded/data.20thC_ReanV2c.html.
Gilleland, E., Katz, R.W., 2011. New software to analyze how extremes change over time. Eos 92 (2), 13–14.
GRDC, Global Runoff Data Center: http://www.bafg.de/GRDC.
Hirahara, S., Ishii, M., Fukuda, Y., 2014. Centennial-scale sea surface temperature analysis and its uncertainty. J. Clim. 27, 57–75.
IPCC, 2013: Summary for policymakers. In: Climate Change 2013: The Physical Science Basis. Contribution of Working Group I to the Fifth Assessment Report of the Intergovernmental Panel on Climate Change [Stocker, T.F., D. Qin, G.-K. Plattner, M. Tignor, S. K. Allen, J. Boschung, A. Nauels, Y. Xia, V. Bex and P.M. Midgley (eds.)]. Cambridge University Press, Cambridge, United Kingdom and New York, NY, USA.
Kalnay, E., et al., 1996. The NCEP/NCAR 40-Year Reanalysis Project. Bull. Am. Meteorol. Soc. 77, 437–471.
Kanamitsu, M., Ebisuzaki, W., Woollen, J., Yang, S.-K., Hnilo, J.J., Fiorino, M., Potter, G.L., 2002. NCEP-DOE AMIP-II Reanalysis (R-2). Bull. Am. Meteorol. Soc. 1631-1643.
Koch, H., Vogele, S., 2009. Dynamic modeling of water demand, water availability and adaptation strategies for power plants to global change. Ecol. Econ. 68, 2031–2039.
Kruger, A., Sekele, S., 2013. Trends in extreme temperature indices in South Africa: 1962–2009. Int. J. Climatol. 33, 661–676.
Kunkel, K. E., et al., 2008: Observed changes in weather and climate extremes. In: Weather and Climate Extremes in a Changing Climate. Regions of Focus: North America, Hawaii, Caribbean, and U.S. Pacific Islands T. R. Karl, G. A. Meehl, D. M. Christopher, S. J. Hassol, A. M. Waple, and W. L. Murray (a report by the U.S. Climate Change Science Program and the Subcommittee on Global Change Research).
Lionello, P. (Ed.), 2012. The Climate of the Mediterranean Region, From the Past to the Future. Elsevier, Amsterdam, Netherlands.
Ludwig, R., Roson, R., 2016. Climate change, water and security in the Mediterranean. Sci. Total Environ. 543, 847–850 (Introduction to the special issue).
Ludwig, R., Roson, R., Zografos, C., Kallis, G., 2011. Towards an inter-disciplinary research agenda on climate change, water and security in southern Europe and neighboring countries. Environ. Sci. Pol. 14, 794–803.
Majone, B., Villa, F., Deidda, R., Bellin, A., 2016. Impact of climate change and water use policies on hydropower potential in the south-eastern Alpine region. Sci. Total Environ. 543 (B), 965–980.
Matzarakis, A., Nastos, P.T., 2011. Human-biometeorological assessment of heat waves in Athens. Theor. Appl. Climatol. 105 (1e2), 99e106.
McNeill, I. A century of Irish summers. http://climate.arm.ac.uk/publications/IMcN.pdf.
New, M., et al., 2006. Evidence of trends in daily climate extremes over southern and west Africa. J. Geophys. Res. Atmos. 111, D14102.
Parker, D.E., 2011. Recent land surface air temperature trends assessed using the 20th Century Reanalysis. J. Geophys. Res. 116, D20125.
Perkins, S.E., Alexander, L.V., 2012. On the measurement of heat waves. J. Clim. 26, 4500–4517.
Perkins, S.E., Alexander, L.V., Nairn, J.R., 2012. Increasing frequency, intensity and duration of observed global heatwaves and warm spells. Geophys. Res. Lett. 39, L20714.
Peterson, T.C., Zhang, X.B., Brunet-India, M., Vazquez-Aguirre, J.L., 2008. Changes in North American extremes derived from daily weather data. J. Geophys. Res. Atmos. 113, D07113.
Peterson, T.C., et al., 2013. Monitoring and understanding changes in heat waves, cold waves, floods and droughts in the United States: state of knowledge. Bull. Am. Meteorol. Soc. 94, 821–834.
Rahimzadeh, F., Asgari, A., Fattahi, E., 2009. Variability of extreme temperature and precipitation in Iran during recent decades. Int. J. Climatol. 29, 329–343.
Rinaudo, J.D., Neverre, N., Montginoul, M., 2012. Simulating the impact of pricing policies on residential water demand: a Southern France case study. Water Resour. Manag. 26 (7), 2057e2068.
Russo, S., Dosio, A., Graversen, R.G., Sillmann, J., Carrao, H., Dunbar, M.B., Singleton, A., Montagna, P., Barbola, P., Vogt, J.V., 2014. Magnitude of extreme heat waves in present climate and their projection in a warming world. J. Geophys. Res. Atmos. 119, 12500–12512.
Russo, S., Sillmann, J., Fischer, E., 2015. Top ten European heatwaves since 1950 and their occurrence in the coming decades. Environ. Res. Lett. 10, 124003.
Scanlon, B., Duncan, I., Reedy, R., 2013. Drought and the water-energy nexus in Texas. Environ. Res. Lett. 8, 045033.
Seneviratne, S.I., Corti, T., Davin, E.L., Hirschi, M., Jaeger, E.B., Lehner, I., Orlowsky, B., Teuling, A.J., 2010. Investigating soil moisture-climate interactions in a changing climate: a review. Earth Sci. Rev. 99 (3–4), 125–161.
Seneviratne, S.I., Nicholls, N., Easterling, D., Goodess, C.M., Kanae, S., Kossin, J., Luo, Y., Marengo, J., McInnes, K., Rahimi, M., Reichstein, M., Sorteberg, A., Vera, C., Zhang, X., 2012. Changes in climate extremes and their impacts on the natural physical environment. In: Field, C.B., Barros, V., Stocker, T.F., Qin, D., Dokken, D.J., Ebi, K.L., Mastrandrea, M.D., Mach, K.J., Plattner, G.-K., Allen, S.K., Tignor, M., Midgley, P.M. (Eds.), Managing the Risks of Extreme Events and Disasters to Advance Climate Change Adaptation. Cambridge University Press, Cambridge, UK, and New York, NY, USA, pp. 109–230 (A Special Report of Working Groups I and II of the Intergovernmental Panel on Climate Change (IPCC)).
Skansi, M., et al., 2013. Warming and wetting signals emerging from analysis of changes in climate extreme indices over South America. Glob. Planet. Chang. 100, 295–307.
Strengers, Y., 2012. Peak electricity demand and social practice theories: reframing the role of change agents in the energy sector. Energ Policy 44, 226e234.
Tryhorn, L., Risbey, J., 2006. On the distribution of heat waves over the Australian region. Aust. Meteorol. Mag. 55, 169–182.
Uppala, S.M., KÅllberg, P.W., Simmons, A.J., Andrae, U., Bechtold, V.D.C., Fiorino, M., Gibson, J.K., Haseler, J., Hernandez, A., Kelly, G.A., Li, X., Onogi, K., Saarinen, S., Sokka, N., Allan, R.P., Andersson, E., Arpe, K., Balmaseda, M.A., Beljaars, A.C.M., Berg, L.V.D., Bidlot, J., Bormann, N., Caires, S., Chevallier, F., Dethof, A., Dragosavac, M., Fisher, M., Fuentes, M., Hagemann, S., Hólm, E., Hoskins, B.J., Isaksen, L., Janssen, P.A.E.M., Jenne, R., Mcnally, A.P., Mahfouf, J.-F., Morcrette, J.-J., Rayner, N.A., Saunders, R.W., Simon, P., Sterl, A., Trenberth, K.E., Untch, A., Vasiljevic, D., Viterbo, P., Woollen, J., 2005. The ERA-40 re-analysis. Q.J.R. Meteorol. Soc. 131, 2961–3012. http://dx.doi.org/10.1256/qj.04.176.
van den Hurk, B., Best, M., Dirmeyer, P., Pitman, A., Polcher, J., et al., 2011. Acceleration of land surface model development over a decade of glass. Bulletin of the American Meteorological Society 92 (12), 1593–1600.
van Vliet, M.T.H., Vogele, S., Rubbelke, D., 2013. Water constraints on European power supply under climate change: impacts on electricity prices. Environ. Res. Lett. 8 (2013), 035010 (10pp).
Vautard, R., Honor'e, C., Beekman, M., Rouil, L., 2005. Simulation of ozone during heat wave and emission control scenarios. Atmos. Environ. 39, 2957–2967.
Vautard, R., Yiou, P., D'Andrea, F., de Noblet, N., Viovy, N., Cassou, C., Polcher, J., Ciais, P., Kageyama, M., Fan, Y., 2007. Summertime European heat and drought waves induced by wintertime Mediterranean rainfall deficit. Geophys. Res. Lett. 34, L07711.
Wang, G., Dolman, S.J., Alessandri, A., 2011. A summer climate regime over Europe modulated by the North Atlantic Oscillation. Hydrol. Earth Syst. Sci. 15, 57–64.
Wetz, M.S., Yoskowitz, D.W., 2013. An 'extreme' future for estuaries? Effects of extreme climatic events on estuarine water quality and ecology. Mar. Pollut. Bull. 69 (1e2), 7e18.
WHO (World Health Organisation), 2004. Heat-Waves: Risks and Responses (Denmark: Copenhagen) p. 124.
WHO (World Health Organisation), 2010. Wildfires and Heat-Wave in the Russian Federation (Denmark: Copenhagen) p. 17.
WMO, 2011. World's 10th Warmest Year, Warmest Year With La Niña Event, Lowest Arctic Sea Ice Volume. Press Release No. 935. WMO, Geneva.
Woodruff, S.D., Worley, S.J., Lubker, S.J., Ji, Z., Freeman, J.E., Berry, D.I., Brohan, P., Kent, E.C., Reynolds, R.W., Smith, S.R., Wilkinson, C., 2011. ICOADS Release 2.5: extensions and enhancements to the surface marine meteorological archive. Int. J. Climatol. 31, 951–967 (CLIMAR-III Special Issue).
Zamboni, L., Cherchi, A., Carril, A.F., n. Characterizations of Heat Waves: An Example for La Plata Basinwww.mcs.anl.gov/papers/P3006-0712.pdf.
Zampieri, M., D'Andrea, F., Vautard, R., Ciais, P., de Noblet-Ducoudre, N., Yiou, P., 2009. Hot European summers and the role of soil moisture in the propagation of Mediterranean drought. J. Clim. 22, 4747–4758.
Zampieri, M., Scoccimarro, E., Gualdi, S., 2013. Atlantic influence on spring snowfall over Alps in the last 150 years. Environ. Res. Lett. 8 (3). http://dx.doi.org/10.1088/1748-9326/8/3/034026.
Zampieri, M., Scoccimarro, E., Gualdi, S., Navarra, A., 2015. Observed shift towards earlier spring discharge in the main Alpine rivers. Sci. Total Environ. 503–504, 222–232.